THEMIS multipoint observations of Pi2 pulsations inside and outside the plasmasphere

H. Luo,[1,2] G. X. Chen,[1] A. M. Du,[1] V. Angelopoulos,[3] W. Y. Xu,[1] X. D. Zhao,[1] and Y. Wang[1]

[1]   Much evidence indicates that Pi2 pulsations in the inner magnetosphere can be explained as radially trapped fast-mode waves in the plasmasphere. Most of these studies, however, are based on observations from a single spacecraft in the plasmasphere and low-latitude ground stations within several hours of local time. Here we present simultaneous observations of two Pi2 pulsations on 26 January 2009 by three THEMIS probes (P3, P4, and P5) and the Ascension Island (ASC) ground station ($L \sim 1.002$, MLT ~ 23). By using plasma density and spacecraft potential measurements, we determined that during this time P4 and P5 were located inside the plasmasphere and P3 was located outside it. It is found that fast-mode components (compressional component Bz, azimuthal component Ey) observed by P4 and P5 have a high correlation with the H component at ASC while those at P3 do not. The Bz oscillations at P4 are nearly in phase with ground Pi2 while those at P5 near the plasmapause are almost out of phase with the H component on the ground during the two Pi2 events. The Ey-H cross phases at P4 and P5 are nearly constant at $-90°$ for both Pi2 events. These multipoint observations strongly suggest that fast-mode waves trapped in the plasmasphere are the source of the low-latitude Pi2 pulsations.

1.   Introduction

[2]   Pi2 pulsations, which can be indicators of a substorm onset [*Saito*, 1969; *Saito et al.*, 1976], are damped oscillations of the geomagnetic field in the 40–150 s period band. They occur at all latitudes on the nightside and exhibit latitudinal and longitudinal amplitude and phase variations [*Yumoto*, 1986]. Maximum amplitudes of Pi2 pulsations are usually observed in the region of the auroral zone beneath the substorm-enhanced ionospheric electrojet [e.g., *Olson and Rostoker*, 1975]. These auroral zone Pi2s have been interpreted as transient Alfvén waves; their period is determined by the Alfvén wave travel time between the ionosphere and the near-Earth plasma sheet [e.g., *Baumjohann and Glassmeier*, 1984]. At midlatitude nightside, Pi2s are clearly observed to have similar signatures extending over at least 60° longitude near the meridian of the substorm current wedge (SCW) [*Singer et al.*, 1983]; their polarization pattern varies systematically relative to the center of the substorm current wedge [*Lester et al.*, 1983]. Therefore, the SCW model is favored to explain the generation of midlatitude Pi2s. Pi2s can be observed at almost all local times and even on the dayside in midlatitudes to low latitudes [*Sutcliffe and Yumoto*, 1989, 1991]. Shear Alfvén mode resonances [*Tamao*, 1965; *Chen and Hasegawa*, 1974a; *Southwood*, 1974], surface waves excited on the plasmapause [*Chen and Hasegawa*, 1974b; *Sutcliffe*, 1975], bursty bulk flow- (BBF-) driven model [*Kepko and Kivelson*, 1999; *Kepko et al.*, 2001], and cavity mode resonances [e.g., *Saito and Matsushita*, 1968] have been proposed as possible generation mechanisms of Pi2 pulsations in midlatitudes to low latitudes.

[3]   The oscillatory nature of Pi2 pulsations has usually been attributed to magnetohydrodynamic standing waves, which can be excited by compressional hydromagnetic waves [*Dungey*, 1954]. Both shear Alfvén waves and compressional fast-mode waves can produce standing waves in the magnetosphere. These waves, either Alfvén or magnetosonic, can be excited by impulsive hydromagnetic momentum released when the near-Earth ($R \leq 10\ R_E$) magnetotail goes through a rapid configurational change at the expansion phase onset of a substorm [*Southwood and Stuart*, 1980]. The damping rate of Alfvén waves (which propagate along the background magnetic field) is regulated by ionospheric conductivity [*Takahashi et al.*, 1996]. However, the damping rate of magnetosonic waves (which propagate isotropically) is controlled by not only the ionospheric conductivity but

---

[1]Institute of Geology and Geophysics, Chinese Academy of Sciences, Beijing, China.
[2]Graduate University of Chinese Academy of Sciences, Beijing, China.
[3]Institute of Geophysics and Planetary Physics, University of California, Los Angeles, California, USA.

also by the radial distribution of the Alfvénic velocity [*Fujita and Glassmeier*, 1995].

[4] Although the field line resonance (FLR) model can successfully explain the variation of Pi2 pulsation amplitude with latitude and the associated latitudinal variation of wave polarization [*Samson et al.*, 1971], it cannot account for frequent observations of the same discrete frequencies over a wide range of latitudes in the inner magnetosphere and on the ground. *Kivelson and Southwood* [1985] proposed that the discrete frequencies correspond to eigenfrequencies of the fast (compressional) mode in the magnetosphere. *Kivelson and Southwood* [1986] found that in a box model the eigenmode equation yields a spectrum of discrete eigenfrequencies. For nightside Pi2s at low latitudes, both observations [e.g., *Lester and Orr*, 1983; *Yeoman and Orr*, 1989; *Takahashi and Anderson*, 1992; *Takahashi et al.*, 1992, 1995; *Keiling et al.*, 2001] and theoretical model calculations [*Lee*, 1998; *Lee and Kim*, 1999; *Fujita et al.*, 2002] support cavity mode resonance or virtual trapped resonance as the generation mechanism. Other studies [e.g., *Han et al.*, 2004] found that Pi2 pulsations at low-latitude dayside cannot be simply explained by the global cavity resonance, and they suggested these Pi2s were generated by the current flows in the E region along the equator. *Kim et al.* [2010] found that plasmaspheric cavity resonance might not establish itself globally because of strong longitudinal attenuation of fast-mode waves near the duskside caused by duskside plasmapause undulations.

[5] Both the plasmaspheric cavity mode and plasmaspheric virtual resonance (PVR) require that fast-mode waves be trapped in the inner magnetosphere and that the radial structures of their fast-mode components (Bz, Ey) be qualitatively the same [*Takahashi et al.*, 2003a]. The difference between the PVR mode and the idealized cavity mode is that the latter requires a perfectly reflecting outer boundary (e.g., plasmapause) while the former allows fast-mode wave energy escapes through the outer boundary. In addition, when realistic plasma, magnetic field configurations are considered, the eigenmode has shorter wavelengths near the outer boundary [*Denton et al.*, 2002; *Takahashi et al.*, 2003a]. As a result, the nodes (antinodes) of both fundamental and second harmonics are located closer to the outer boundary than those in the idealized cavity mode, which was proved by *Takahashi et al.* [2003b], who investigated the radial profile of the phase and amplitude of the Ey and Bz components observed by the CRRES satellite and suggested that the fundamental node of Bz is located inside the plasmasphere near the plasmapause. A node or antinode is a point at which the amplitude of one of the two types of displacement in a standing wave has a minimum or maximum value. *Lee and Lysak* [1999] performed numerical studies that suggested that Pi2 pulsations in the magnetosphere can be explained by the PVR model. *Kim et al.* [2005] gave observational evidence of the PVR model outside the plasmasphere by using the Polar satellite, though the PVR mode events were observed off the equator at ~15° to 60° magnetic latitude. This was further proved by *Teramoto et al.* [2008], who statistically studied the Pi2 pulsations inside and outside the plasmasphere observed by the DE-1 satellite. Recently, *Teramoto et al.* [2011] statistically presented two-satellite observations of the Pi2 pulsations inside and outside the plasmasphere and provided additional

evidence of plasmaspheric virtual resonance. Little clear observational evidence for Pi2-associated fast-mode standing waves in the nightside region near the magnetic equator of the outer magnetosphere (beyond the plasmapause) has been reported, however. *Takahashi et al.* [2001] found that although poloidal components had high coherence with Pi2 pulsations at low latitudes when CRRES was in the plasmasphere, they did not maintain high coherence when the spacecraft moved completely into the plasmatrough. This suggests that the outer boundary of the cavity is the plasmapause. The phase differences between poloidal components and H components at low latitudes for both fundamental and secondary harmonic cavity resonances were investigated extensively by *Takahashi et al.* [2003a].

[6] There are a few studies that used multipoint observations in space and on the ground to examine the spatial structure of Pi2 pulsations both inside and outside the plasmasphere. For example, *Collier et al.* [2006] studied a Pi2 event by using three Cluster satellites inside the plasmasphere and a satellite in the plasmatrough; they gave evidence of standing waves confined in the plasmasphere. Recently, *Teramoto et al.* [2011] statistically presented two-satellite observations of the Pi2 pulsations at different regions in the inner magnetosphere and provided additional evidence of plasmaspheric virtual resonance. However, these studies did not provide a detailed radial structure of plasmaspheric resonance such as the location of the node or antinode for both fundamental and second harmonic structures of the magnetic and electric fields.

[7] In this paper, we present four point observations of Pi2 pulsations in the inner magnetosphere by using three THEMIS probes and a ground magnetic station. Two probes were located inside the plasmasphere, one located near the Earth and the other located near the plasmapause. The third probe was located just outside the plasmapause. We believe that the spatial distribution of observation points can help us study the radial structure of Pi2 pulsations inside and outside the plasmasphere in great detail.

[8] The remainder of this paper is organized as follows. In section 2 we describe the data sets. In section 3 we present observations and data analysis. In section 4, we discuss the results of our observations. In section 5 we give our conclusions.

2. Data Sets

[9] In this study, we use data from identical instruments on THEMIS-A (P5), THEMIS-E (P4), and THEMIS-D (P3) [*Angelopoulos*, 2008; *Sibeck and Angelopoulos*, 2008] and at a low-latitude ground station on Ascension Island (ASC). The THEMIS magnetic data come from the fluxgate magnetometer (FGM) [*Auster et al.*, 2008]. A combination of FGE (engineering, 8 Hz data) and FGL (fast survey product "low" resolution at 4 Hz) from P4 is used to reduce digitization noise in the sub-nanotesla range. Data from FGS are used to study the magnetic oscillations at P3 and P5. The plasma density data are from the electrostatic analyzer (ESA) [*McFadden et al.*, 2008]. The electric field and probe potential data are from the electric field instrument (EFI) [*Bonnell et al.*, 2008]. The THEMIS electric field data used here are spin-fit, 3 s averaged vector samples constructed
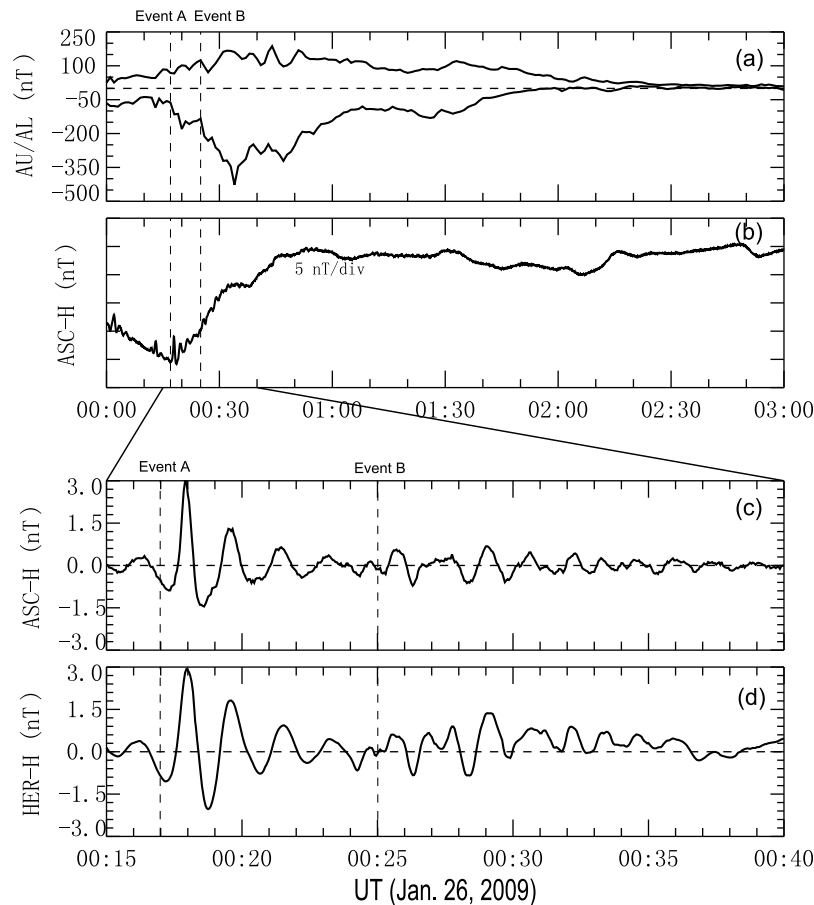
Figure 1. (a) The *AU/AL* index from 0000 to 0300 UT. (b) The *H* component of the Ascension Island station (*L* = 1.002, geographic latitude = −7.9°, and geographic longitude = 345.6°). (c) High pass-filtered data at Ascension Island station. (d) High-pass-filtered data at Hermanus (HER) (*L* = 1.45, geographic latitude = −34.4°, geographic longitude = 19.2°). The vertical dashed lines indicate Pi2 onsets at 0017 UT (event A) and at 0025 UT (event B).

from spin-plane components by assuming no electric field along the background magnetic field ($\mathbf{E}g\mathbf{B} = 0$).

[10] Magnetic and electric fields from THEMIS are resampled to 3 s resolution and rotated into local mean-field-aligned (MFA) coordinates [e.g., *Takahashi et al.*, 1990]. Three components of the magnetic field in the MFA system are $\mathbf{e}_x$, $\mathbf{e}_y$, and $\mathbf{e}_z$, where $\mathbf{e}_z$ is a unit vector parallel to the 5 min sliding average magnetic field direction, $\mathbf{e}_y$ is the unit azimuthal component parallel to the vector product of the probe position vector and the $\mathbf{e}_z$ vector, and $\mathbf{e}_x$ is the unit radial component, completing the right-hand rule. After that rotation, the data are operated by a 3 s averaged field minus a 5 min averaged field and high-pass filtered with a 150 s period.

[11] Data from a three-components suspended fluxgate magnetometer sampled every second from the Ascension Island observatory are used to identify the low-latitude Pi2 pulsations. ASC was located at −2.6° of the geomagnetic latitude, 57.2° geomagnetic longitude. Measurements at Hermanus (HER) performed by the induction magnetometer are used to compare the pulsations with those from ASC to confirm that the equatorial anomalous behavior of the Pi2 pulsations does not appear at the ASC station. We have

taken 3 s running averages of the 1 s resolution data into 3 s resolution to make the data resolution comparable to the THEMIS field data.

3. Data Presentation

[12] In this section we present data analysis details. Two Pi2 events that occurred from 0015 to 0040 UT on 26 January 2009 are described, including the positions of three THEMIS probes relative to the plasmapause and the field components inside and outside the plasmasphere.

3.1. Overview

[13] Figure 1 shows an overview of geomagnetic conditions from 0000 to 0300 UT. The *AU* and *AL* indices (Figure 1a) begin to increase and decrease sharply, respectively, at about 0017 UT. Another sharp decrease of the *AL* index occurs at about 0025 UT; the index reaches its minimum value (∼−430 nT) at about 0034 UT, indicating a moderate substorm. The THEMIS pseudo-*AE* index (which has more stations at this time; not shown) shows similar behavior. Los Alamos National Laboratory geostationary particle data (http://leadbelly.lanl.gov/lanl_ep_data/) also indicate

energetic particle injections, which confirm the occurrence of a substorm. The H component magnetic field data from ASC are plotted in Figure 1b. The H component began to increase almost simultaneously with the AL index decrease at 0017 UT, indicating a positive bay excursion. These are typical substorm signatures of nightside low-latitude stations. During the H component increase, two Pi2 onsets were observed at about 0017 and 0025 UT; these could be clearly seen superposed on the H component of the magnetic field observed at the ASC station. Therefore, the two Pi2 events in our study are substorm-related phenomena.

[14] Ground signatures of Pi2 pulsations in the daytime near the magnetic equator usually exhibit characteristics similar to those of the polar Pi2 pulsations [*Yumoto and CPMN Group*, 2001]. During the Pi2 events in our study, the Ascension observatory was located in the nighttime, so the equatorial anomalous behavior of the Pi2 pulsations may not appear at this observatory. We compare the Pi2s at both ASC and Hermanus (HER) to confirm this. In Figures 1c and 1d, we plot high-pass-filtered H components from the ASC and HER stations, respectively. As we can see in the two panels, nearly the same waveforms appear in the two observatories. During this time, ASC ($L = 1.002$, magnetic latitude $= -2.47°$, and magnetic local time $= 23$ h) was located at the vicinity of the geomagnetic equator and HER ($L = 1.45$, magnetic latitude $= -34.02°$, and magnetic local time $= 0.8$ h) was located at midlatitude about 2 h east of the ASC station. Similar behavior between the two observatories means that the equatorial anomalous behavior of the Pi2 pulsations does not appear at the ASC station, and Pi2 signatures at the ASC stations represent behavior of the Pi2 pulsations in middle and low latitudes other than that of polar Pi2 pulsations.

[15] To investigate the wave mode inside and outside the plasmasphere, we need to identify the location of the plasmapause. Both the plasma density and the spacecraft potential, which depends on the plasma density [*Pedersen et al.*, 1998; *Scudder et al.*, 2000], are used to determine that location. Cross correlation between measured plasma densities and spacecraft potential determined from the THEMIS EFI Langmuir probes provides their quantitative relationship [*Bonnell et al.*, 2008]. The plasma density and the spacecraft potential of P4, P5, and P3 from 0000 to 0200 UT are shown in Figure 2. Ion (black) and electron (green) density measurements are shown in Figure 2a. The ion and electron densities come into agreement at about 0015 UT, 0040 UT, and 0103 UT for P3, P5, and P4, respectively (black dashed line in each panel of Figure 2a). The time is consistent with the sharpest change (red dashed line in each panel of Figure 2b) in the spacecraft potential measurements plotted in Figure 2b. The thick black bar in each panel indicates the time interval of interest (0015 to 0040 UT).

[16] Figure 3 shows the magnetic local time (MLT) and the dipole L distribution of P4, P5, P3, and the low-latitude ASC station from 0000 to 0200 UT on 26 January 2009. During this time, the THEMIS probes were in stage seven of the "tail science phase." P4, P5, and P3 were in an outbound pass near the magnetic equator with magnetic latitudes of 9°, 2°, and 2°, respectively. The solid circles in each line indicate the crossing of the plasmapause by each probe at the

different times identified in Figure 2. The time of interest (0015–0040 UT) is indicated by a thick bar for each probe. During this time, the three probes were located at premidnight, P4 moved outward from $L \sim 2.9$ to $L \sim 3.5$ (MLT from 20.6 to 21.5); P5 moved outward from $L \sim 4.0$ to ~ 4.9 (MLT from 22.3 to 23); and P3 moved outward from $L \sim 5.7$ to ~ 6.2 (MLT from 23.2 to 23.6). The ground ASC station ($L \sim 1.002$) was located near midnight with MLT from 22.8 to 23.2. Both the probes and the ground station were located on the nightside with a small local time separation that was favorable for analyzing the radial mode structure of Pi2 pulsations [*Takahashi et al.*, 1995].

[17] From the analysis above, we can confirm that P3, P5, and P4 crossed the plasmapause at about 0015 UT, 0040 UT, and 0103 UT, respectively. During the two Pi2 events, P4 was inside the plasmasphere closer to the Earth; P5 was also inside the plasmasphere but near the plasmapause; and P3 was outside the plasmasphere.

3.2. Observations of P4 Inside the Plasmasphere Closer to the Earth

[18] For P4 inside the plasmasphere closer to the Earth, we examine the field components of the Pi2 pulsations (0015–0040 UT) and their correlation with observations at the ASC station. Figure 4a shows the MFA components of P4 (from top to bottom, Ex, Ey, Bx, By, Bz) and the H component from ASC observations. Oscillations in the Pi2 band can be clearly seen in the azimuthal component (Ey) of the electric field, the field-aligned component (Bz) of the magnetic field, and the H component of the ASC station. The toroidal components (Ex, By) are smaller than the poloidal components (Ey, Bx, Bz), which implies that the poloidal components dominated the wave mode at P4. This is consistent with a statistical study by *Takahashi et al.* [1995], who concluded that the oscillations were dominated by poloidal components on the nightside at $L < 4$. As shown in Figure 4a (middle and bottom), the time series plots of Bz and H have almost identical waveforms during the two Pi2 events, which implies that Pi2s at P4 and ASC are from the same source. Figure 4b shows the spectral properties of the two Pi2 events, computed by using a fast Fourier transform from the high-pass-filtered data. Figure 4b (top) shows the spectral properties of the poloidal components at P4 and H at ASC for event A, calculated for the 0015–0022 UT interval. It can be seen that poloidal components at P4 and H at ASC have almost identical spectral shapes and have a strong peak at 9.3 mHz. We also note that there is a second peak of the H component at the frequency of 19 mHz, which is not evident of the poloidal components at P4. Figure 4b (bottom) shows the spectral properties of the poloidal components at P4 and H at ASC for event B, calculated for the 0025–0032 UT interval. Similar spectral properties are observed for event B except that the H component shows a second power peak at ~14.2 mHz.

[19] To investigate the radial structure of the fast-mode wave, we examine the coherence and phase difference between poloidal components at P4 and H at ASC. Figure 5 (top) shows the wavelet coherence between Ey at P4 and the H component at ASC. The wavelet coherence finds regions in time-frequency space in which the two time series co-vary (but do not necessarily have high power) [e.g., *Grinsted*
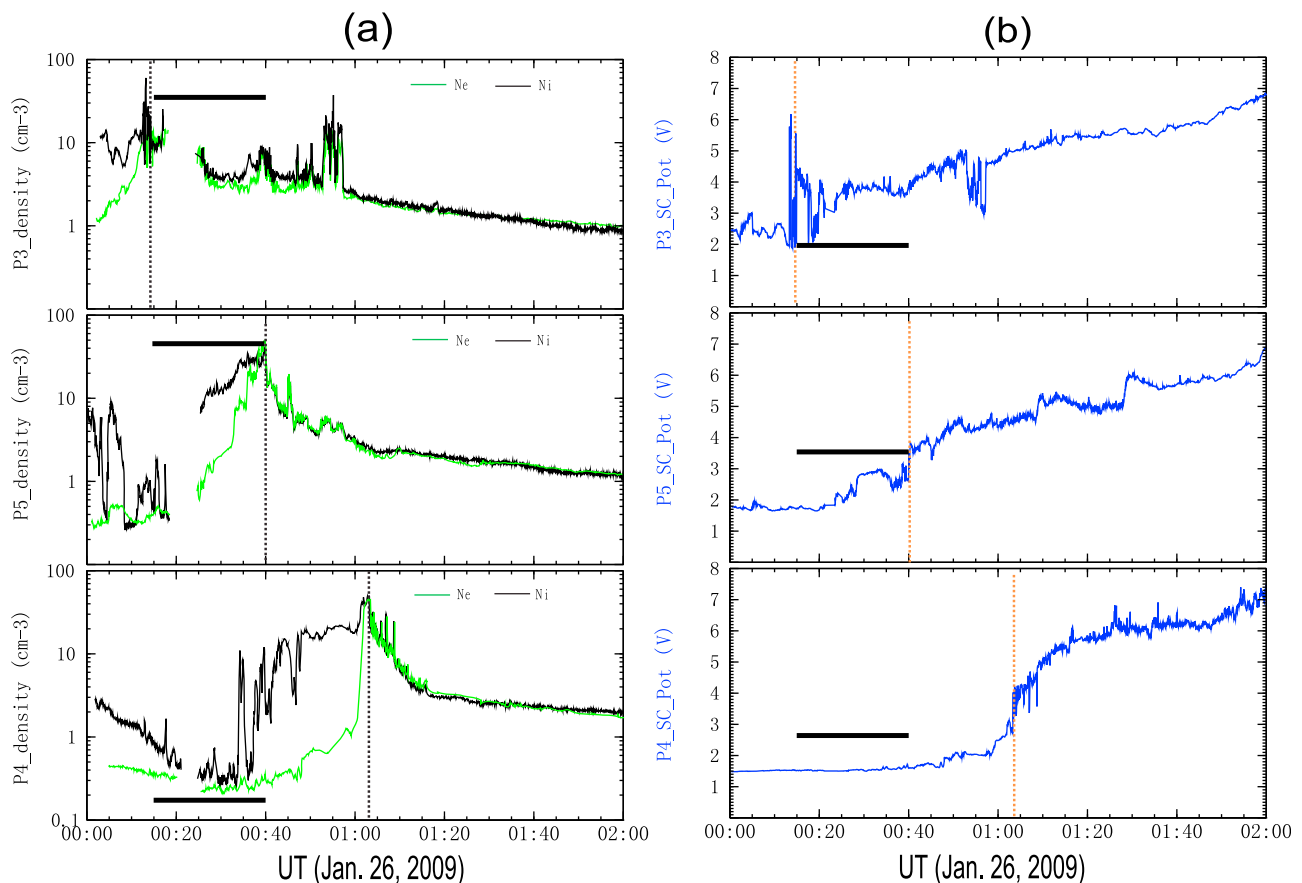
Figure 2. (a) From top to bottom, the ion (black) and electron (green) densities measured by P3, P5, and P4. The horizontal thick black bar stands for the time of interest, and the plasmapause crossing is marked by vertical dashed lines. (b) The format is identical to that of Figure 2a, but for the spacecraft potential measurements.

et al., 2004]. The Ey at P4 is well correlated with the H component during the two Pi2 events, with a wavelet coherence of more than 0.9 in the period band from ~70 to ~130 s centered at ~100 s. The cross phase between Ey and H is nearly −90° for both two Pi2 events (indicated by the phase arrows pointing upward). The Bz-H coherence is shown in Figure 5 (bottom). High Bz-H coherence is also present in the period band from ~70 to ~130 s centered at ~100 s. Bz oscillates in phase with H during 0015–0031 UT (indicated by the phase arrows pointing right). After 0031 UT, the high coherence between Bz and H shifts to a period of ~45 s, and Bz is no longer in phase with the H component (indicated by the phase arrows pointing left) but instead is in antiphase with the H component.

[20] These results are consistent with the fundamental structure of the fast-mode wave trapped in the plasmasphere [*Takahashi et al.*, 2003a]. We can confirm that P4 was located inward of the fundamental Bz node (Ey antinode) during the two Pi2 events.

3.3. Observations of P5 Inside the Plasmasphere Near the Plasmapause

[21] According to the analysis in section 3.1, P5 moved across the plasmapause at ~0040 UT. Therefore, it was located inside the plasmasphere and near the plasmapause
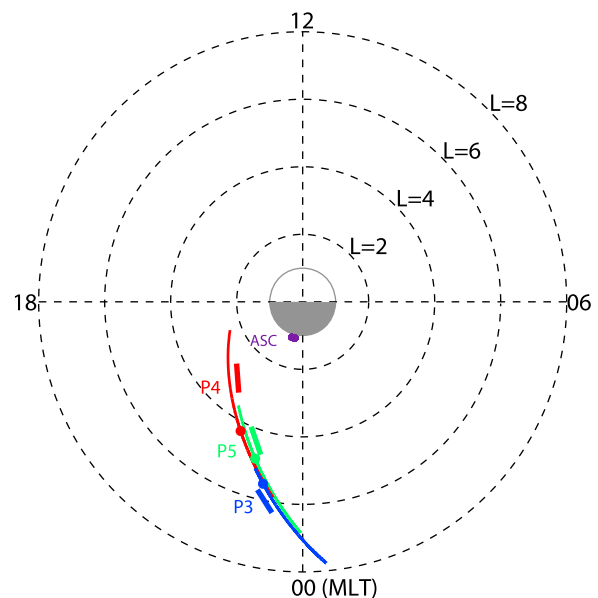

Figure 3. Magnetic local time (MLT) and dipole L distribution of P3, P4, P5, and the ASC station from 0000 to 0200 UT. The solid circle in each line indicates crossing of the plasmapause by each probe. The time period (0015–0040 UT) is marked by the thick bar beside each line.
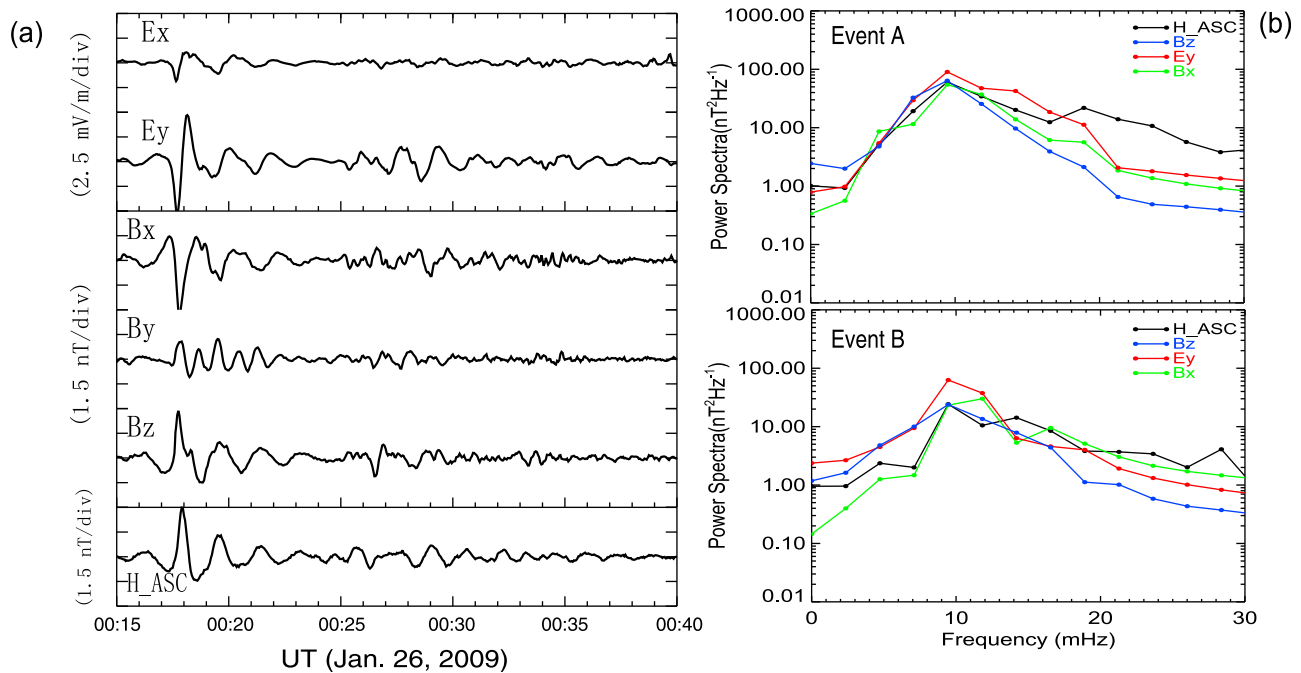
Figure 4. (a) Electric and magnetic oscillations in MFA coordinates at P4 and the *H* component at the ASC station from 0015 to 0040 UT. (b) Spectral properties of the poloidal components (*Bx*, *Bz*, *Ey*) at P4 and the *H* component at ASC during (top) event A and (bottom) event B.

during the two Pi2 events. Midway through this time of interest, P5 was at $L \sim 4.3$, $\sim 2°$ MLAT, and 22.7 h MLT. The ASC station was ~ 0.5 h MLT east of P5. The field components and their correlations with ASC observations are also investigated. Figure 6a shows the field oscillations at P5 and the *H* component at the ASC station from 0015 to 0040 UT. The same coordinate system and data format as in Figure 4a are used. Pulsations in all field components are shown in the Pi2 band and show nonsinusoidal signatures. Unlike the P4 oscillations, both poloidal and toroidal components were observed at P5, and their amplitudes were comparable. The spectral properties of the two Pi2 events are shown in Figure 6b. For event A (Figure 6b, top), both the *Ey* and *H* at ASC show a power peak at 9.3 mHz, while the *Bz* spectrum shows a strong power band from ~ 9 to ~ 19 mHz. Bx has a power peak at ~ 12 mHz, which is a little higher than that of *Ey*. For event B, *Ey* and *Bx* spectra show a strong peak at 9.3 mHz and the *Bz* spectrum shows a peak at 14.2 mHz. The *H* component shows both peaks at 9.3 and 14.2 mHz, which correspond to the *Ey* and *Bz* peaks, respectively.

[22] The wavelet coherence between poloidal components at P5 and the *H* component at ASC for both Pi2 events is shown in Figure 7. Figure 7 (top) demonstrates that *Ey* is well correlated with the *H* component, with a squared wavelet coherence of more than 0.8 in the period centered at ~ 100 s for both Pi2 events. The *Ey*-H cross phase at the period ~ 100 s is about $-90°$ (indicated by the phase arrows pointing upward), which is the same as the cross phase between *Ey* and *H* observed at P4. The *Bz*-H coherence (Figure 7, bottom) shows different signatures from those at P4, which exhibits high correlations at ~ 50 s and ~ 70 s for

events A and B, respectively. In addition, *Bz* oscillations are nearly out of phase with *H* for both Pi2 events.

[23] From the observations at P5 above, we identify that P5 observed the fundamental structure of the *Ey* component and the second harmonic signatures of *Bz* components for both Pi2 events. These results are consistent with the radial structure of the trapped fast-mode wave illustrated in Figure 1 of *Takahashi et al.* [2003a]. In section 4.1, we discuss the structures as well as the position relative to the node or antinode.

3.4. Observations of P3 Outside the Plasmasphere

[24] As shown in Figure 3, P3 moved across the plasma-pause at ~ 0014 UT. At the midpoint of the two Pi2 events, P3 was located at $L \sim 6.1$, $2°$ MLAT, and 23.2 MLT. The ASC station was in nearly the same MLT as that of P3. Figure 8a shows time series plots of the disturbed field components in the MFA system at P3 and the *H* component at ASC. Although oscillations are present at both poloidal and toroidal components, their waveforms are not quite sinusoidal and differ significantly from the pulsations at P4 and P5. Although the first two cycles of the *Bz* at P3 mat-ched those of the *H* component at ASC to some extent, a good, long-lasting match, like those observations at P4 and P5 inside the plasmasphere, did not happen at P3. Figure 8b (top) shows that the power spectra of poloidal components exhibit signatures that are somewhat similar to those of the *H* component for event A at ~ 9 mHz; there is no similar spectral shape for event B (Figure 8b, bottom). The *Ey*-H and *Bz*-H coherences are rather low for both Pi2 events (Figure 9).
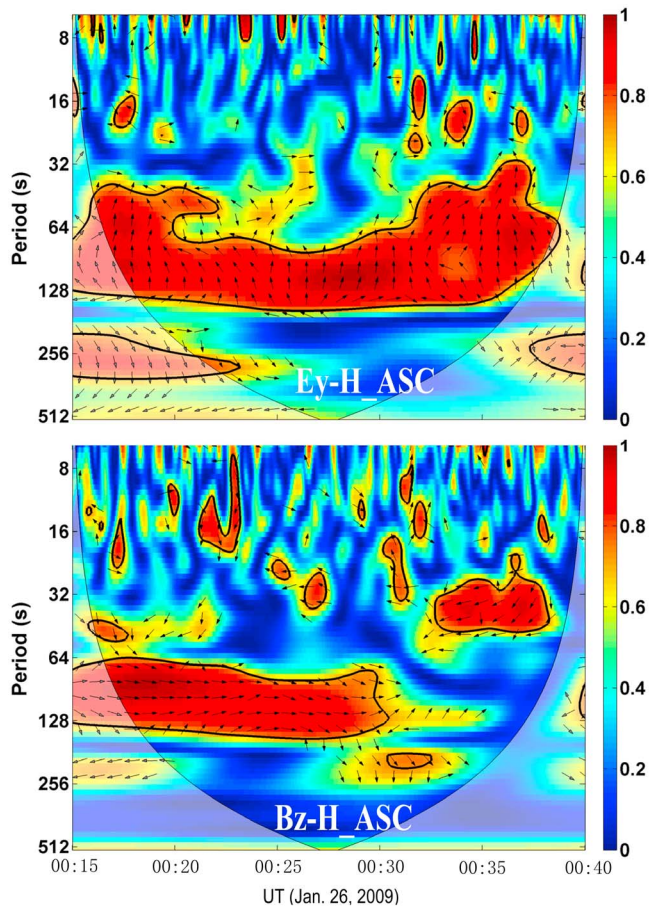
Figure 5. (top) The squared wavelet coherence between the compressional component (*Bz*) at P4 and the *H* component at the ASC station. (bottom) Azimuthal component (*Ey*) and *H* component. The 5% significance level against red noise is shown as a thick contour. The relative phase relationship is shown as arrows (with in-phase pointing right, antiphase pointing left, −90° cross phase marked by pointing upward).

[25] Observations at P3 imply that the low-latitude ground Pi2 may not be directly excited by the fast-mode wave outside the plasmasphere. The plasmapause provides an adequate barrier for trapping fast-mode waves.

4. Discussion

[26] In the previous section, we discussed wave modes for two Pi2 events observed by three THEMIS probes inside and outside the plasmasphere and their relationship to low-latitude ground Pi2. The wave modes of the three probes and the probe-ground coherences are highly dependent on the positions of the probes relative to the plasmapause. This dependence is consistent with the findings of *Takahashi et al.* [2001].

4.1. What Causes Frequency Differences in the Cavity?

[27] The resonance period of the fundamental mode (Pi2 period) can be approximately expressed as $T_{Pi2} = 2R_E \int_{L_0}^{L_{pp}} \frac{dx}{V_A(x)}$, where $V_A(x) = \frac{B(x)}{\sqrt{\mu_0 \rho}}$ (Alfvénic velocity) is a

function of the radial distance (*x*) [*Takahashi et al.*, 2010]; the integration is made from the inner boundary (L_0) to the outer boundary (L_{pp}). Hence, the wave period of Pi2 pulsations exhibited by plasmaspheric cavity resonance depends on the size and density of the plasmasphere. For an idealized situation, the frequency of the second harmonic normalized to the fundamental equals two.

[28] In Figure 1 of *Takahashi et al.* [2003a], they summarized the radial structure of the fundamental and second harmonics of the cavity model. They assume that the mode is excited between two rigid radial boundaries that would correspond to the equatorial ionosphere and plasmapause, respectively. Considering an idealized cavity, both harmonics have *Ey* nodes located at two boundaries and the *Bz* node is located at the *Ey* antinode and vice versa. A node or antinode is a point at which the amplitude of one of the two types of displacement in a standing wave has the minimum or maximum value. For the fundamental mode, there are three nodes or antinodes in the plasmasphere with *Ey* −90° out of phase with the *H* component while *Bz* is in phase with the *H* inside the *Bz* node and anti phase with *H* outside the *Bz* node. For the second harmonic mode, there are five locations of nodes or antinodes in the plasmasphere, with three *Bz* antinodes located at two boundaries and in the middle of the cavity (labeled L_{n2}); while two nodes are located in the middle of two adjacent nodes, which are labeled L_{n1} and L_{n3} in Figure 1 of *Takahashi et al.* [2003a], respectively. *Ey* is ± 90° out of phase with *Bz*. We also should note that the nodes (antinodes) of both fundamental and second harmonics are located closer to the outer boundary than those in Figure 1 of *Takahashi et al.* [2003a] because the eigenmode has shorter wavelengths near the outer boundary when a realistic plasma, magnetic field configuration, and energy leakage through the boundaries are considered [*Denton et al.*, 2002; *Takahashi et al.*, 2003a].

[29] For event A (0017 to 0024 UT), the 9.3 mHz oscillation was observed at P4 in both *Bz* and *Ey* (see Figure 4b). Poloidal components have high coherence with *H* at ASC in the period band around 100 s (see Figure 5). At P5, the 9.3 mHz oscillation was observed only in the *Ey* component while the *Bz* showed strong power at 9–19 mHz and centered at ~14 mHz (Figure 6b). Both frequencies were detected in the *H* component at the ASC station. This difference could also be seen in the satellite-ground coherence (Figure 7). Observations for event B also show similar results.

[30] It is reasonable to explain the frequency difference of field components between P4 and P5 to be that the two probes located at different positions of the cavity observed different harmonics and the ASC station observed both harmonics. We can infer that the plasmapause was located at $L \sim 5.6$ according to the positions where P3 and P5 crossed the plasmapause during the midpoint of the two Pi2 events. P4 ($L \sim 2.8$) was possibly located between L_{n1} and L_{n2} and near L_{n1}, which is the *Bz* node of the second harmonic. Therefore, it mainly observed the fundamental mode of *Bz*. P5 was possible located near L_{n2}, which is the second harmonic antinode (fundamental node) of *Bz*. Hence, *Bz* mainly exhibited the second harmonic signature. However, we could not identify which side L_{n2} P5 was located on in our observations. *Ey* oscillations at P5 exhibited only the fundamental mode structure since the *Ey*-*H* coherence is rather low at the second harmonic frequency (Figure 7, top)
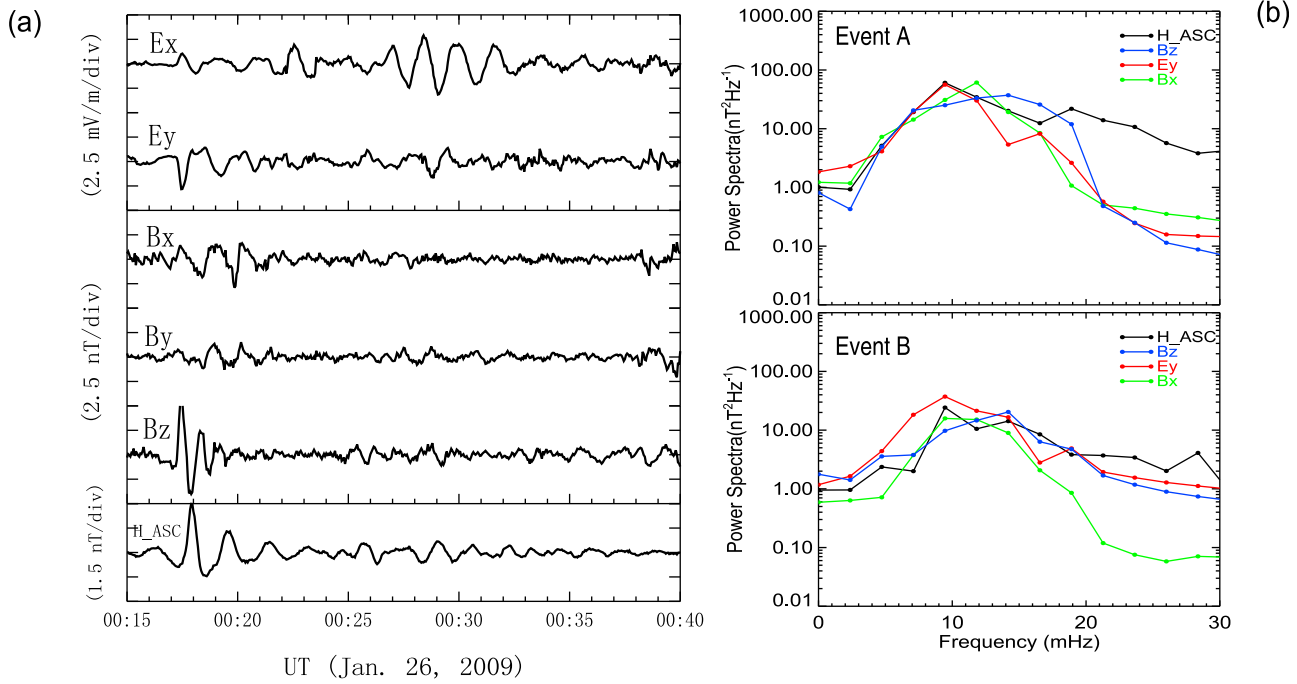
Figure 6. The format is identical to that of Figure 4, but for P5 observations.

because the amplitude of Ey at the second harmonic frequency is small near L_{n2}. According to radial structure of both harmonics [*Takahashi et al.*, 2003a, Figure 1], we could identify only that P5 was located near L_{n2}.

[31] It was found that the frequencies of the second harmonic oscillations had different values (19 mHz for event A, 14.2 mHz for event B) while the fundamental frequencies were the same for events A and B. A possible explanation was that the frequencies of both fundamental and second harmonic were changed from event to event. Unlike the idealized situation, the $f2/f1$ ratios do not equal two and are not stable in the realistic plasmasphere. *Takahashi et al.* [2003a] studied two successive Pi2 events and found that the $f2/f1$ ratios were 1.7 and 2.2, respectively. Statistical studies of the harmonic Pi2 events on the ground also reported a large spread in the frequency ratio [*Denton et al.*, 2002, summary table]. In our study, the frequency ratios showed 2.0 ($f2$ = 19 mHz, $f1$ = 9.3 mHz) and 1.5 ($f2$ = 14.2 mHz, $f1$ = 9.3 mHz) for events A and B, respectively. The two frequency ratios were in reasonable range according to *Denton et al.* [2002].

[32] We also note that the Bz-H coherence at P4 during 0033–0037 UT showed high correlations at ~ 45 s (Figure 5, bottom). At first, we thought that P4 observed the second harmonic of Bz oscillations for event B. However, we noted that event B ended at about 0034 UT. In fact, the amplitudes of poloidal oscillations at both P4 and P5 were rather small after 0032 UT compared with those of events A and B. Hence, we cannot attribute the 45 s correlations between Bz and H after 0032 UT to P4 observing the second harmonic structure of event B.

4.2. Comparison of the Observations With Other Models

[33] Although many studies show that theoretical or observational plasmaspheric wave trapping is the main generation
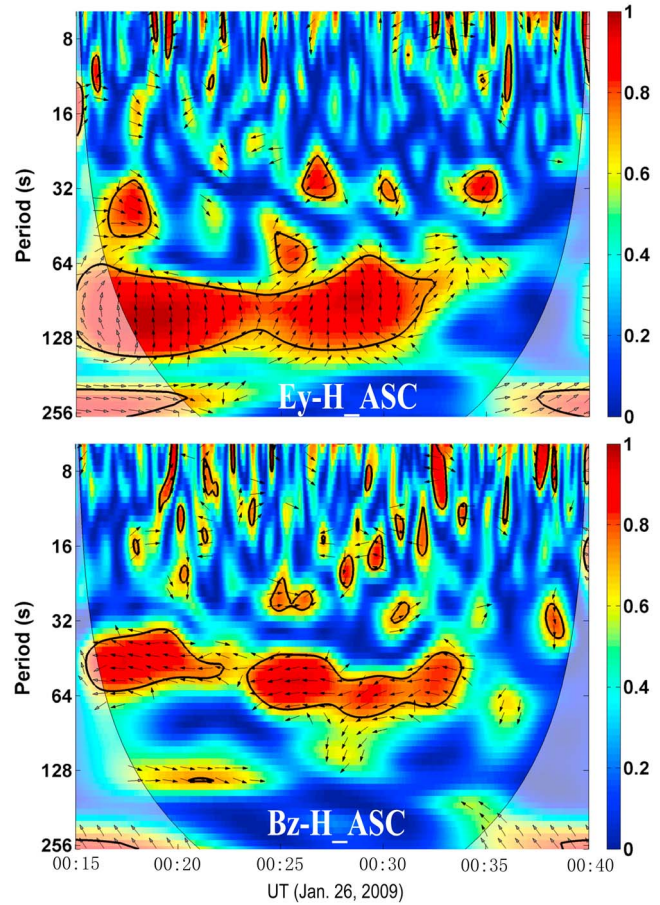

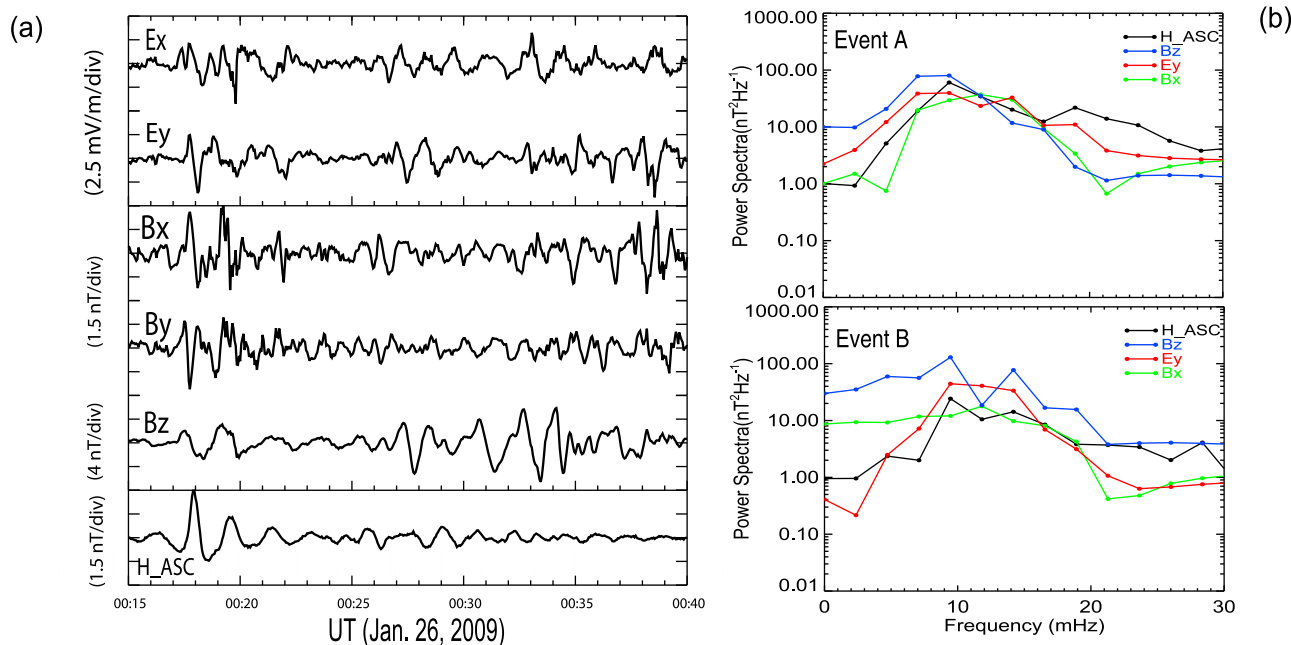**Figure 7.** The format is identical to that of Figure 5, but for P5 observations.

Figure 8. The format is identical to that of Figure 4, but for P3 observations.

mechanism of low-latitude Pi2 pulsations, its occurrence in the real magnetosphere is not universally accepted. A major question is that of the relative importance of external forcing waves and internal resonance in establishing the frequency of the Pi2 pulsations in the inner magnetosphere. It was discovered that the waveforms of low-latitude Pi2s matched well with the time-delayed earthward ion bulk flows [*Kepko and Kivelson*, 1999; *Kepko et al.*, 2001]. This led them to suggest that Pi2 pulsations at low-latitude nightside and flanks are directly driven by time-modulated earthward fast flows. These periodical fast flows reach the dipolar inner magnetosphere and enhance periodic compressional pulses, which travel earthward and generate Pi2s at nightside and flanks of the Earth with possible mode conversions.

[34] An important feature in our study is that there are three probes making simultaneous observations near the magnetic equator inside and outside the plasmasphere. This can help us identify the source of Pi2 events. For event A, although the first two wave cycles observed by P3 outside the plasmasphere show some similarity to those inside the plasmasphere and ASC station, we cannot attribute it to be BBF driven. If the Pi2 pulsations in the plasmasphere are directly driven by an external source such as BBF, the amplitude of the compressional pulses outside the plasmasphere may larger than that inside it. However, we notice that the *Bz* amplitude (7 nT peak to peak; see Figure 8a) at P3 is smaller than that at P5 (9 nT peak to peak; see Figure 6a). In addition, if the *Ey* Pi2 pulsations observed in the plasmasphere resulted from radially propagating fast-mode waves, the phase would change linearly with *L*. However, the cross phase between the azimuthally components (*Ey*) inside the plasmasphere (see Figure 5 (top) and Figure 7 (top)) and the *H* component is nearly constant at −90°. Therefore, Pi2s in our study may not be caused by simple radial propagation. The BBF-driven model is not appropriate for event A. For event B, although the *Bz*
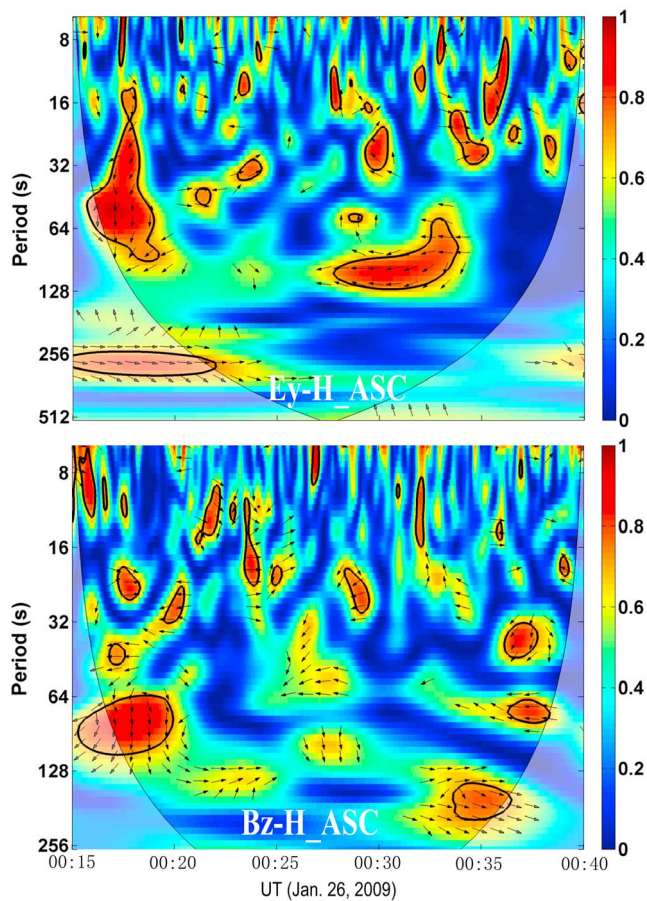

Figure 9. The format is identical to that of Figure 5, but for P3 observations.

amplitude at P3 is much larger than that inside the plasmasphere and at ground, the waveforms between *Bz* at P3 and the *H* component at ASC are quite different and their coherence is rather low (<0.6). Hence, event B also cannot be explained by the BBF-driven model.

[35] At first we attempt to explain the matching between *Bz* and *H* for the first two cycles of event A by the PVR model. According to the numerically simulated PVR [*Teramoto et al.*, 2011], the *Bz* node is located around the inner edge of the plasmapause. If event A exhibits the PVR mode at P3, the *Bz* oscillations should be out of phase with ground *H* because P3 was outside the *Bz* node. However, we note that the cross phase between them is about 90° during 00:17–00:20 UT (see Figure 9, bottom), which seems not to be consistent with the PVR model. We believe this does not contradict the PVR model. *Teramoto et al.* [2011] showed that high-coherence *Bz* events detected by CCE were limited to the time when CCE was in the low-latitude near-Earth region because the PVR mode was substantially attenuated at the region outside the plasmasphere, not far from the plasmapause. The PVR mode at P3 may be masked by the compressional oscillations driven by the free energy in the plasma sheet during substorm onset [*Kim et al.*, 2005]. We also examined the Poynting flux at P5 and P3 (not shown). The radial component of the Poynting flux showed an outward and inward net energy flux at P5 and P3, respectively. For a plasmaspheric virtual resonance (PVR) mode, the Pi2 is excited inside the plasmasphere and the wave energy can escape through the plasmapause because the plasmapause is not a perfect outer boundary. Hence, there should be an outward radial Poynting flux at P5 inside the plasmasphere near the plasmapause and at P3 just outside the plasmapause. This is the case with the observations at P5, but not the case at P3. This confirmed that the PVR mode signature outside the plasmapause was masked by strong non-Pi2 disturbances [e.g., *Takahashi et al.*, 1995].

5. Conclusions

[36] In this study, we examined simultaneous observations of two Pi2 pulsations by three THEMIS probes (P3, P4, and P5) that were located at premidnight and by a low-latitude ground station (Ascension Island). From the observations and analysis above, several conclusions can be drawn.

[37] 1. Three probes across the plasmapause at different times were identified by using plasma density and spacecraft potential measurements: 0015 UT, 0040 UT, and 0103 UT for P3, P5, and P4, respectively. During the two Pi2 events, P4 and P5 were inside the plasmasphere, with P4 closer to the Earth and P5 near the plasmapause; P3 was outside the plasmapause. The low-latitude ground station, Ascension Island, was located within several hours in MLT of the three probes.

[38] 2. Fast-mode components observed by P4 in the plasmasphere closer to the Earth have high coherence with the *H* component of the ASC station for the two Pi2 events. The cross phases between the fast-mode components (*Bz*, *Ey*) and the *H* component at ASC are 0° and −90°, respectively.

[39] 3. Fast-mode components observed by P5 near the plasmapause also have high coherence with the *H* component of the ASC station. The fundamental was observed in the electric azimuthal component while the second harmonic was observed in the magnetic compressional component of the cavity mode.

[40] 4. Field oscillations at P3, outside the plasmasphere, do not show a good, long-lasting match, like those observations at P4 and P5 inside the plasmasphere, with ground Pi2.

[41] 5. Radially trapped fast-mode waves in the plasmasphere (plasmaspheric cavity resonance or plasmaspheric virtual resonance) are the source of nightside low-latitude Pi2 pulsations, and the plasmapause is the most likely outer boundary for the fast-mode wave trapping.

References

Angelopoulos, V. (2008), The THEMIS mission, *Space Sci. Rev.*, *141*, 5–34, doi:10.1007/s11214-008-9336-1.

Auster, H. U., et al. (2008), The THEMIS fluxgate magnetometer, *Space Sci. Rev.*, *141*, 235–264, doi:10.1007/s11214-008-9365-9.

Baumjohann, W., and K.-H. Glassmeier (1984), The transient response mechanism and Pi2 pulsations at substorm onset—Review and outlook, *Planet. Space Sci.*, *32*, 1361–1370, doi:10.1016/0032-0633(84)90079-5.

Bonnell, J. W., F. S. Mozer, G. T. Delory, A. J. Hull, R. E. Ergun, C. M. Cully, V. Angelopoulos, and P. R. Harvey (2008), The electric field instrument (EFI) for THEMIS, *Space Sci. Rev.*, *141*, 303–341, doi:10.1007/s11214-008-9469-2.

Chen, L., and A. Hasegawa (1974a), A theory of long-period magnetic pulsations: 1. Steady state excitation of field line resonance, *J. Geophys. Res.*, *79*, 1024–1032, doi:10.1029/JA079i007p01024.

Chen, L., and A. Hasegawa (1974b), A theory of long-period magnetic pulsations: 2. Impulse excitation of surface eigenmode, *J. Geophys. Res.*, *79*, 1033–1037, doi:10.1029/JA079i007p01033.

Collier, A. B., A. R. W. Hughes, L. G. Blomberg, and P. R. Sutcliffe (2006), Evidence of standing waves during a Pi2 pulsation event observed on Cluster, *Ann. Geophys.*, *24*, 2719–2733, doi:10.5194/angeo-24-2719-2006.

Denton, R. E., D. H. Lee, K. Takahashi, J. Goldstein, and R. Anderson (2002), Quantitative test of the cavity resonance explanation of plasmaspheric Pi2 frequencies, *J. Geophys. Res.*, *107*(A7), 1093, doi:10.1029/2001JA000272.

Dungey, J. W. (1954), Electrodynamics of the outer atmosphere, *Sci. Rep. 69*, Pa. State Univ., State College, Pa.

Fujita, S., and K.-H. Glassmeier (1995), Magnetospheric cavity resonance oscillations with energy flow across the magnetopause, *J. Geomag. Geoelectr.*, *47*, 1277–1292, doi:10.5636/jgg.47.1277.

Fujita, S., H. Nakata, M. Itonaga, A. Yoshikawa, and T. Mizuta (2002), A numerical simulation of the Pi2 pulsations associated with the substorm current wedge, *J. Geophys. Res.*, *107*(A3), 1034, doi:10.1029/2001JA900137.

Grinsted, A., J. C. Moore, and S. Jevrejeva (2004), Application of the cross wavelet transform and wavelet coherence to geophysical time series, *Nonlinear Processes Geophys.*, *11*, 561–566, doi:10.5194/npg-11-561-2004.

Han, D.-S., T. Iyemori, M. Nosé, H. McCreadie, Y. Gao, F. Yang, S. Yamashita, and P. Stauning (2004), A comparative analysis of low-latitude Pi2 pulsations observed by Ørsted and ground stations, *J. Geophys. Res.*, *109*, A10209, doi:10.1029/2004JA010576.

Keiling, A., J. R. Wygant, C. Cattel, K.-H. Kim, C. T. Russell, D. K. Milling, M. Temerin, F. S. Mozer, and C. A. Kletzing (2001), Pi2 pulsations observed with the Polar satellite and ground stations: Coupling of trapped

and propagating fast mode waves to a midlatitude field line resonance, *J. Geophys. Res.*, *106*, 25,891–25,904, doi:10.1029/2001JA900082.

Kepko, L., and M. Kivelson (1999), Generation of Pi2 pulsations by bursty bulk flows, *J. Geophys. Res.*, *104*, 25,021–25,034, doi:10.1029/1999JA900361.

Kepko, L., M. G. Kivelson, and K. Yumoto (2001), Flow bursts, braking, and Pi2 pulsations, *J. Geophys. Res.*, *106*, 1903–1915, doi:10.1029/2000JA000158.

Kim, K.-H., D.-H. Lee, K. Takahashi, C. T. Russell, Y.-J. Moon, and K. Yumoto (2005), Pi2 pulsations observed from the Polar satellite outside the plasmapause, *Geophys. Res. Lett.*, *32*, L18102, doi:10.1029/2005GL023872.

Kim, K.-H., H.-J. Kwon, D.-H. Lee, H. Jin, K. Takahashi, V. Angelopoulos, J. W. Bonnell, K. H. Glassmeier, Y.-D. Park, and P. Sutcliffe (2010), A comparison of THEMIS Pi2 observations near the dawn and dusk sectors in the inner magnetosphere, *J. Geophys. Res.*, *115*, A12226, doi:10.1029/2010JA016010.

Kivelson, M. G., and D. J. Southwood (1985), Resonant ULF waves: A new interpretation, *Geophys. Res. Lett.*, *12*, 49–52, doi:10.1029/GL012i001p00049.

Kivelson, M. G., and D. J. Southwood (1986), Coupling of global magnetospheric MHD eigenmodes to field line resonances, *J. Geophys. Res.*, *91*, 4345–4351, doi:10.1029/JA091iA04p04345.

Lee, D.-H. (1998), On the generation mechanism of Pi2 pulsations in the magnetosphere, *Geophys. Res. Lett.*, *25*, 583–586, doi:10.1029/98GL50239.

Lee, D.-H., and K. Kim (1999), Compressional MHD waves in the magnetosphere: A new approach, *J. Geophys. Res.*, *104*, 12,379–12,385, doi:10.1029/1999JA900053.

Lee, D.-H., and R. Lysak (1999), MHD waves in a three-dimensional dipolar magnetic field: A search for Pi2 pulsations, *J. Geophys. Res.*, *104*, 28,691–28,699, doi:10.1029/1999JA900377.

Lester, M., and D. Orr (1983), Correlations between ground observations of Pi2 geomagnetic pulsations and satellite plasma density observations, *Planet. Space Sci.*, *31*, 143–160, doi:10.1016/0032-0633(83)90050-8.

Lester, M., J. W. Hughes, and H. J. Singer (1983), Polarization patterns of Pi 2 magnetic pulsations and the substorm current wedge, *J. Geophys. Res.*, *88*, 7958–7966, doi:10.1029/JA088iA10p07958.

McFadden, J., C. Carlson, D. Larson, J. Bonnell, F. Mozer, V. Angelopoulos, K.-H. Glassmeier, and U. Auster (2008), THEMIS ESA first science results and performance, *Space Sci. Rev.*, *141*, 477–508, doi:10.1007/s11214-008-9433-1.

Olson, J. V., and G. Rostoker (1975), Pi2 pulsations and the auroral electrojet, *Planet. Space Sci.*, *23*, 1129–1139, doi:10.1016/0032-0633(75)90163-4.

Pedersen, A., F. Mozer, and G. Gustafsson (1998), Electric field measurements in a tenuous plasma with spherical double probes, in *Measurement Techniques in Space Plasmas: Fields*, Geophys. Monogr. Ser., vol. 103, edited by R. F. Pfaff et al., pp. 1–12, AGU, Washington, D. C., doi:10.1029/GM103p0001.

Saito, T. (1969), Geomagnetic pulsations, *Space Sci. Rev.*, *10*, 319–412, doi:10.1007/BF00203620.

Saito, T., and S. Matsushita (1968), Solar cycle effects on geomagnetic Pi 2 pulsations, *J. Geophys. Res.*, *73*, 267–286, doi:10.1029/JA073i001p00267.

Saito, T., K. Yumoto, and Y. Koyama (1976), Magnetic pulsation Pi2 as a sensitive indicator of magnetic substorm, *Planet. Space Sci.*, *24*, 1025–1029, doi:10.1016/0032-0633(76)90120-3.

Samson, J. C., J. A. Jacobs, and G. Rostoker (1971), Latitude-dependent characteristics of long-period geomagnetic micropulsations, *J. Geophys. Res.*, *76*, 3675–3683, doi:10.1029/JA076i016p03675.

Scudder, J. D., X. Cao, and F. S. Mozer (2000), Photoemission current-spacecraft voltage relation: Key to routine, quantitative low-energy plasma measurements, *J. Geophys. Res.*, *105*, 21,281–21,294, doi:10.1029/1999JA900423.

Sibeck, D. G., and V. Angelopoulos (2008), THEMIS science objectives and mission phases, *Space Sci. Rev.*, *141*, 35–59, doi:10.1007/s11214-008-9393-5.

Singer, H. J., W. J. Hughes, P. F. Fougere, and D. J. Knecht (1983), The localization of Pi2 pulsations: Ground-satellite observations, *J. Geophys. Res.*, *88*, 7029–7036, doi:10.1029/JA088iA09p07029.

Southwood, D. J. (1974), Some features of field line resonances in the magnetosphere, *Planet. Space Sci.*, *22*, 483–491, doi:10.1016/0032-0633(74)90078-6.

Southwood, D. J., and W. F. Stuart (1980), Pulsations at the substorm onset, in *Dynamics of the Magnetosphere*, edited by S.-I. Akasofu, pp. 341–355, D. Reidel, Norwell, Mass.

Sutcliffe, P. R. (1975), The association of harmonics in Pi2 power spectra with the plasmapause, *Planet. Space Sci.*, *23*, 1581–1587, doi:10.1016/0032-0633(75)90085-9.

Sutcliffe, P. R., and K. Yumoto (1989), Dayside Pi 2 pulsations at low latitudes, *Geophys. Res. Lett.*, *16*, 887–890, doi:10.1029/GL016i008p00887.

Sutcliffe, P. R., and K. Yumoto (1991), On the cavity mode nature of low-latitude Pi2 pulsations, *J. Geophys. Res.*, *96*, 1543–1551, doi:10.1029/90JA02007.

Takahashi, K., and B. J. Anderson (1992), Distribution of ULF energy ($f < 80$ mHz) in the inner magnetosphere: A statistical analysis of AMPTE CCE magnetic field data, *J. Geophys. Res.*, *97*, 10,751–10,773, doi:10.1029/92JA00328.

Takahashi, K., R. W. McEntire, A. T. Y. Lui, and T. A. Potemra (1990), Ion flux oscillations associated with a radially polarized transverse Pc 5 magnetic pulsation, *J. Geophys. Res.*, *95*, 3717–3731, doi:10.1029/JA095iA04p03717.

Takahashi, K., S. Ohtani, and K. Yumoto (1992), AMPTE CCE observations of Pi 2 pulsations in the inner magnetosphere, *Geophys. Res. Lett.*, *19*, 1447–1450, doi:10.1029/92GL01283.

Takahashi, K., S. Ohtani, and B. J. Anderson (1995), Statistical analysis of Pi2 pulsations observed by the AMPTE CCE spacecraft in the inner magnetosphere, *J. Geophys. Res.*, *100*, 21,929–21,941, doi:10.1029/95JA01849.

Takahashi, K., B. J. Anderson, and S. Ohtani (1996), Multisatellite study of nightside transient toroidal waves, *J. Geophys. Res.*, *101*, 24,815–24,825, doi:10.1029/96JA02045.

Takahashi, K., S. Ohtani, W. J. Hughes, and R. R. Anderson (2001), CRRES observation of Pi2 pulsations: Wave mode inside and outside the plasmasphere, *J. Geophys. Res.*, *106*, 15,567–15,581, doi:10.1029/2001JA000017.

Takahashi, K., R. R. Anderson, and W. J. Hughes (2003a), Pi2 pulsations with second harmonic: CRRES observations in the plasmasphere, *J. Geophys. Res.*, *108*(A6), 1242, doi:10.1029/2003JA009847.

Takahashi, K., D.-H. Lee, M. Nosé, R. R. Anderson, and W. J. Hughes (2003b), CRRES electric field study of the radial mode structure of Pi2 pulsations, *J. Geophys. Res.*, *108*(A5), 1210, doi:10.1029/2002JA009761.

Takahashi, K., et al. (2010), Multipoint observation of fast mode waves trapped in the dayside plasmasphere, *J. Geophys. Res.*, *115*, A12247, doi:10.1029/2010JA015956.

Tamao, T. (1965), Transmission and coupling resonance of hydromagnetic disturbances in the non-uniform Earth's magnetosphere, *Sci. Rep., ser. 5, Geophysics*, vol. 17, pp. 43–72, Tohoku Univ., Tohoku, Japan.

Teramoto, M., M. Nosé, and P. R. Sutcliffe (2008), Statistical analysis of Pi2 pulsations inside and outside the plasmasphere observed by the polar orbiting DE-1 satellite, *J. Geophys. Res.*, *113*, A07203, doi:10.1029/2007JA012740.

Teramoto, M., K. Takahashi, M. Nosé, D.-H. Lee, and P. R. Sutcliffe (2011), Pi2 pulsations in the inner magnetosphere simultaneously observed by the Active Magnetospheric Particle Tracer Explorers/Charge Composition Explorer and Dynamics Explorer 1 satellites, *J. Geophys. Res.*, *116*, A07225, doi:10.1029/2010JA016199.

Yeoman, T. K., and D. Orr (1989), Phase and spectral power of mid-latitude Pi2 pulsations: Evidence for a plasmaspheric cavity resonance, *Planet. Space Sci.*, *37*, 1367–1383, doi:10.1016/0032-0633(89)90107-4.

Yumoto, K. (1986), Generation and propagation mechanisms of low latitude magnetic pulsations: A review, *J. Geophys.*, *60*, 79–105.

Yumoto, K., and CPMN Group (2001), Characteristics of Pi2 geomagnetic pulsations observed at the CPMN stations: A review of the STEP results, *Earth Planets Space*, *53*, 981–992.

V. Angelopoulos, Institute of Geophysics and Planetary Physics, University of California, Los Angeles, CA 92093, USA.

G. X. Chen, A. M. Du, H. Luo, Y. Wang, W. Y. Xu, and X. D. Zhao, Institute of Geology and Geophysics, Chinese Academy of Sciences, Beijing 100029, China. (luohao06@gmail.com)